Journal of Neurochemistry, 2007, **101**, 841–853 doi:10.1111/j.1471-4159.2007.04472.x

A human neuronal tissue culture model for Lesch-Nyhan disease

Thomas L. Shirley,* J. Chris Lewers,* Kiyoshi Egami,* Alokes Majumdar,† Mairead Kelly,‡ Irene Ceballos-Picot,‡ Michael M. Seidman† and H. A. Jinnah*

**Department of Neurology, Johns Hopkins University, Baltimore, Maryland, USA*

†*Laboratory of Molecular Gerontology, National Institute on Aging, National Institutes of Health, Baltimore, Maryland, USA*

‡*Department of Biology, Necker-Enfants Malades Hospital and Faculté de Médecine René Descartes, Paris, France*

Abstract

Mutations in the gene encoding the purine salvage enzyme, hypoxanthine–guanine phosphoribosyltransferase (HPRT) cause Lesch-Nyhan disease, a neurodevelopmental disorder characterized by cognitive, neurological, and behavioral abnormalities. Despite detailed knowledge of the enzyme's function, the key pathophysiological changes that accompany loss of purine recycling are unclear. To facilitate delineating the consequences of HPRT deficiency, four independent HPRT-deficient sublines of the human dopaminergic neuroblastoma, SK-N-BE(2) M17, were isolated by targeted mutagenesis with triple helix-forming oligonucleotides. As a group, these HPRT-deficient cells showed several significant abnormalities: (i) impaired purine recycling with accumulation of hypoxanthine, guanine, and xanthine, (ii) reduced guanylate energy charge and GTP : GDP ratio, but normal adenylate energy charge and no changes in any adenine nucleotide ratios, (iii) increased levels of UTP and $NADP^+$, (iv) reduced DOPA decarboxylase, but normal monoamines, and (v) reduction in cell soma size. These cells combine the analytical power of multiple lines and a human, neuronal origin to provide an important tool to investigate the pathophysiology of HPRT deficiency.

Keywords: high performance liquid chromatography, hypoxanthine–guanine phosphoribosyltransferase, Lesch-Nyhan disease, monoamines, purines, triple helix-forming oligonucleotides.

J. Neurochem. (2007) **101**, 841–853.

Hypoxanthine–guanine phosphoribosyltransferase (HPRT) is a ubiquitously expressed enzyme that plays an important salvage role in purine metabolism. It recycles the purine bases, hypoxanthine and guanine, into their corresponding nucleotides, IMP and GMP. Loss of this enzyme in humans causes Lesch-Nyhan disease (LND), which is characterized by dystonia, cognitive impairment, and aggressive and self-injurious behaviors (Schretlen *et al*. 2001; Schretlen *et al*. 2005; Jinnah *et al*. 2006). Many studies have attempted to link the neurobehavioral syndrome with changes in purine homeostasis resulting from loss of purine salvage, but a lack of consistency has made it difficult to definitively identify the most relevant of these changes. Other studies have linked the neurobehavioral syndrome with changes in basal ganglia dopamine neurons, but the link between purines and dopamine systems has not been elucidated (Visser *et al*. 2000).

Tissue culture models have provided important insights into the pathophysiology of many diseases, and several investigators have evaluated a variety of HPRT-deficient ($HPRT^-$) cells for this purpose. The majority of these studies have focused on cells that are easily obtained from patients, such as erythrocytes, lymphocytes, and fibroblasts (Jinnah and Friedmann 2000). These studies have been useful for documenting the biochemical consequences of loss of HPRT function.

Some studies have sought to more closely model the neurobiological consequences of the enzyme defect by studying $HPRT^-$ sublines of neuroblastoma or glioma cells. These studies have provided results, such as changes in

Received October 12, 2006; revised manuscript received November 14, 2006; accepted November 15, 2006.

Address correspondence and reprint requests to H. A. Jinnah, Johns Hopkins Department of Neurology, Meyer Room 6-181, 600 North Wolfe Street, Baltimore, MD 21287, USA. E-mail: hjinnah@jhmi.edu

Abbreviations used: 3-MT, 3-methoxytyramine; 5-HIAA, 5-hydroxyindole acetic acid; 6TG, 6-thioguanine; AEC, adenylate energy charge; DDC, DOPA decarboxylase; DPBS, Dulbecco's phosphate-buffered saline; FBS, fetal bovine serum; GAPDH, gylceraldehyde-3-phosphate dehydrogenase; GEC, guanylate energy charge; HPRT, hypoxanthine–guanine phosphoribosyltransferase; $HPRT^-$, HPRT-deficient; HVA, homovanillic acid; LND, Lesch-Nyhan disease; PCA, perchloric acid; PDT, population doubling time; SDS, sodium dodecyl sulfate; TFO, triple helix-forming oligonucleotide.

neurite number or morphology, which could not have been obtained with non-neural cells. Only a few studies have specifically examined the influence of HPRT deficiency on dopaminergic cells *in vitro*; all of them in rodent models (Bitler and Howard 1986; Yeh *et al*. 1998; Boer *et al*. 2001; Smith and Friedmann 2004).

To explore the consequences of impaired purine recycling in a human dopaminergic neuronal model, four HPRT$^-$ sublines were generated from SK-N-BE(2) M17 neuroblastomas utilizing targeted mutation of HPRT (Puri *et al*. 2002). This cell line was originally explanted from a bone marrow biopsy (Biedler and Spengler 1976) and subcloned by limiting dilution. The M17 subline has many characteristics of an immature dopamine neuron, including expression of enzymes responsible for dopamine synthesis and catabolism (Ciccarone *et al*. 1989; Baptista *et al*. 2003).

Experimental procedures

Cell culture

SK-N-BE(2) M17 cells (ATCC, Manassas, VA, USA) were cultured at 37°C with 5% CO_2 in RPMI 1640 media supplemented with 15% fetal bovine serum (FBS) and 2 mmol/L L-glutamine. All reagents were obtained from Invitrogen (Carlsbad, CA, USA).

Targeted mutation of hypoxanthine–guanine phosphoribosyltransferase

Deletions in the HPRT gene were introduced by mutagenesis of a psoralen cross-link targeted to a site immediately adjacent to exon 5 by a triple helix-forming oligonucleotide (TFO) (Richards *et al*. 2005). Briefly, cells were electroporated with the psoralen-linked TFO and after 3 h were exposed to ultraviolet A light (365 nm, 1.8 J/cm^2, 3 min). The cells were cultured for 7 days and then selected in 6-thioguanine (6TG).

Cellular proliferation

Population doubling times (PDTs) were estimated according to established procedures (Freshney 2000). Briefly, cells were plated in 24-well plates at densities of 1×10^5, 3×10^4, and 1×10^4 cells per well in triplicate. Cells were counted at daily intervals with a hemocytometer after trypan-blue staining. The PDT was estimated by linear regression during the exponential growth phase.

Morphology

For each cell line, 20 phase-contrast digital micrographs were taken of random fields with a Nikon Eclipse TE200-U microscope equipped with an RT Monochrome camera (Diagnostic Instruments, Sterling Heights, MI, USA). Images were imported into NeuroLucida (5.05.4; MicroBrightfield, Williston, VT, USA) and all isolated cells appearing in each image were traced using a Wacom Intuos 2 digitizing tablet (Wacom, Vancouver, WA, USA). Clumped or otherwise obscured cells were excluded to assure unequivocal identification of the cell outline and all processes. At least 100 cells were evaluated for each line.

Several morphometric parameters were quantified using NeuroExplorer (3.70.2; MicroBrightfield) including cellular cross-sectional area, cellular perimeter, and the number, diameter, and length of neurites. Cellular extensions greater than one cell diameter in length were classified as neurites.

Table 1 PCR primers

Gene	Sequence (5′–3′)	T_m	Amplicon
COMT	GGACAGTGCTACTGGCTGAC	62.2	107
	CAGGAACGATTGGTAGTGTGTG	60.9	
DDC	ACACAGGCCGCTATCATGG	61.8	103
	TGGCTTTTAATTTCACTCCACCA	60.4	
GAPDH	GAGCCAAAAGGGTCATCATC	63.3	226
	CCATCCACAGTCTTCTGGGT	64.0	
TH	CTACCAAGACCAGACGTACCA	60.6	91
	GATGCGTGAGGCATAGCTCC	62.8	
VMAT2	GTCACCGGGAATGCTACCAG	62.3	137
	AGACCAACTTGCACGTTTTCA	60.6	

Gene-specific primer pairs were designed using Primerbank (pga.mgh.harvard.edu/primerbank). COMT, catechol-O-methyltransferase; DDC, DOPA decarboxylase; GAPDH, glyceraldehyde-3-phosphate dehydrogenase; TH, tyrosine hydroxylase; T_m, melting temperature; VMAT2, vesicular monoamine transporter 2.

Quantitative PCR

Qiagen's RNeasy Midi Kit (Qiagen, Hilden, Germany) and DNase treatment were used to extract total RNA from $\sim 2 \times 10^7$ cells from each M17 line. First-strand synthesis was performed with 1 μg total RNA, random hexamer primers, and Reverse-IT RTase Blend (ABgene, Epsom, UK).

For quantitative PCR, gene-specific primers (sequence melting temperature (T_m) and amplicon length provided in Table 1) were used with the LightCycler FastStart DNA Master^{PLUS} SYBR Green I kit (Roche Applied Science, Mannheim, Germany). Each reaction was performed in quadruplicate for each line. Data were normalized to GAPDH expression.

Monoamines

Each cell line was allowed to grow to near-confluency. The medium was then replaced with RPMI 1640 with 15% dialyzed FBS and 2 mmol/L glutamine. After 24 h, the conditioned medium was removed, and debris and any suspended cells pelleted. A 900-μL aliquot of the supernatant was then combined with 0.1 mL of 1 mol/L perchloric acid (PCA; Aldrich, St Louis, MO, USA). The attached cells were detached with trypsin and pelleted. After washing in 37°C Dulbecco's phosphate-buffered saline (DPBS), cells were resuspended in 0.1 mol/L PCA and stored at -80°C.

Thawed media and cell lysates were centrifuged at 10 000 *g* for 10 min at 4°C to sediment precipitated proteins. Insoluble material in the supernatant was removed by filtration through 0.45 μm spin filters (Alltech, Nicholasville, KY, USA) and monoamine concentrations determined by reverse-phase HPLC with electrochemical detection, as previously described (Jinnah *et al*. 1999). Protein pellets were dissolved in 2% sodium dodecyl sulfate (SDS) and quantified by bicinchoninic acid (BCA) assay (Pierce, Rockford, IL, USA).

Purines

Hypoxanthine–guanine phosphoribosyltransferase enzyme activity and *de novo* purine synthesis were assessed in live cells by

adaptation of previous methods (Wood *et al*. 1973; Snyder *et al*. 1978). For HPRT activity, the parent and each of the mutant sublines were incubated in suspension (1.5×10^6 cells per 500 μL medium) with 25 μmol/L: ^{14}C-hypoxanthine (40 μCi/mL; Sigma, St Louis, MO, USA) for 60 min at 37°C. For assessment of *de novo* purine synthesis, cells were pulse-labeled in a 6-well format with 25 μmol/L ^{14}C-glycine (40 μCi/mL; Sigma) for 90 min at 37°C. After labeling, cells were washed in DPBS and purines extracted with 50 μL of 0.1 mol/L PCA. A single freeze per thaw cycle (-80°C) preceded pelleting of cellular debris (10 000 *g* for 10 min).

To capture nucleotides, 2.5 μL of the supernatant was spotted per well of a Millipore MultiScreen plate containing diethylaminoethyl anion exchange paper and allowed to adsorb for 1 h. The plate was then washed once with 300 μL of H_2O and three times with 50% methanol. The filters were counted using an LS 6500 Multi-Purpose Scintillation Counter (Beckman Coulter, Fullerton, CA, USA). Protein pellets were dissolved in 2% SDS and quantified by BCA assay.

For quantification of purine pools, samples were prepared as described for monoamines. Prior to filtration, supernatants were neutralized with 2.5% (v/v) 3.5 mol/L potassium carbonate, incubated on ice for 10 min, and the potassium perchlorate precipitate pelleted at 10 000 *g* for 10 min at 4°C.

Purine concentrations were determined by reverse-phase, ion pair HPLC using an Atlantis dC18 column and a 2996 photodiode array detector (Waters, Milford, MA, USA), with most analytes measured at 254 nm. The flow rate was 1 mL/min, with a mobile phase mixture of buffer A: 10 mmol/L ammonium acetate and 2 mmol/L tetratbutylammonium phosphate (pH 5.0) and buffer B: 10 mmol/L ammonium phosphate, 2 mmol/L tetrabutylammonium phosphate (pH 7.0), and 25% acetonitrile. The first 10 min of each run consisted of 100% buffer A and 0% buffer B. The percentage of buffer B then increased linearly to 75% over 15 min and remained at 75% for 10 min. It then increased linearly to 100% buffer B over 5 min and remained at 100% for 15 min. The column was then re-equilibrated in 100% buffer A for 15 min prior to the next run.

Data analysis

For each result set, the parent M17 and each HPRT$^-$ subline were compared utilizing one-way ANOVA with *post hoc* Tukey *t*-tests. Neurite counts and neurite branch order were assessed by Kruskal–Wallis one-way ANOVA. This approach allowed us to identify differences between individual HPRT$^-$ sublines and the parent line, as well as differences between the sublines. However, one-way ANOVA did not provide a suitable means of evaluating the overall effects of HPRT deficiency. To address this, the overall effect of HPRT deficiency was determined by single-sample *t*-test (two-tailed) comparing the means of each subline ($n = 4$) with the mean of the parent line. This approach could not be used for non-continuous measures, as equivalent non-parametric methods require at least six values.

Results

Generation of HPRT-deficient M17 sublines

Four sublines of 6TG-resistant M17 cells were isolated by TFO-mediated mutagenesis of the HPRT gene. This method enriched for HPRT mutations and made 6TG selection possible at the low plating density required to mitigate the bystander effect of metabolic cooperativity (Furth *et al*. 1981). All four sublines had a genomic deletion encompassing all or part of exon 5 (Table 2).

Table 2 Hypoxanthine–guanine phosphoribosyltransferase

Line	Deletion	Enzyme activity	%	*p*-value
M17	NA	1.89 ± 0.08	100	NA
M17^{TG1}	31 613–31 625	0.01 ± 0.01	0.3	<0.0001
M17^{TG3}	31 603–31 956	0.00 ± 0.00	0.2	<0.0001
M17^{TG6}	31 598–31 946	0.02 ± 0.01	1.1	<0.0001
M17^{TG8}	31 602–31 667	0.00 ± 0.00	0.0	<0.0001

Mutations in HPRT$^-$ M17 sublines were mapped to GenBank accession number M26434 (exon 5 spans bases 31 618–31 635). Enzyme activity is expressed as incorporation of 25 μmol/L ^{14}C-hypoxanthine (nmol/mg/h ± SEM) normalized to cellular protein and percent of control ($n = 6$). *Post hoc* results for comparison of parent and each subline by ANOVA ($F = 589.89$; $p < 0.0001$) are shown in final column. A single-sample *t*-test comparing all HPRT$^-$ lines to the parent was also significant ($p < 0.0001$). NA, not applicable.

Hypoxanthine–guanine phosphoribosyltransferase activity

The loss of HPRT function was confirmed by measurement of live culture incorporation of ^{14}C-hypoxanthine into IMP and derivative nucleotides. The parent M17 line readily incorporated ^{14}C-hypoxanthine, while each of the HPRT$^-$ sublines exhibited enzyme activity that was at or below detectable limits (Table 2); consistent with the null phenotype predicted by exon 5 deletion. The rate of *de novo* purine synthesis was also evaluated. The parent M17 line incorporated ^{14}C-glycine at a rate of 67.6 ± 6.1 pmol/mg protein/h, while the individual mutant lines ranged from 42.8 ± 7.9 to 131.9 ± 10.6 pmol/mg/h.

Proliferation rates

To determine if HPRT deficiency impaired cellular proliferation, the PDT during exponential growth was calculated. The average PDT for the parent M17 cells was 27.6 ± 5.2 h. The PDT of individual HPRT$^-$ sublines varied from 29.6 ± 4.5 h to 47.6 ± 9.1 h. The average of all sublines was 39.6 ± 4.6 h (Table 3). Although the HPRT$^-$ sublines showed trends toward slower growth, both one-way ANOVA and single-sample *t*-test did not reveal any significant differences.

Morphology

All of the cell lines appeared healthy without overt signs of toxicity, such as a high frequency of non-viable cells, debris, or apoptotic figures (Fig. 1). Gross morphology for all HPRT$^-$ sublines was similar to that of the parent line. However, one-way ANOVA revealed that three of the

Table 3 Proliferation rates

Line	PDT	Change (%)
M17	27.6 ± 5.2	NA
$M17^{TG1}$	47.4 ± 12.5	73.7
$M17^{TG3}$	33.7 ± 3.8	22.2
$M17^{TG6}$	29.6 ± 4.5	7.3
$M17^{TG8}$	47.6 ± 9.1	72.3

Proliferation rate expressed as population doubling time (PDT; h/division ± SEM) and percent change compared with control ($n = 3$ replicates for each line). PDT was not significantly different in the HPRT$^-$ lines by either ANOVA ($F = 1.552$, $p = 0.261$), or single-sample *t*-test ($p = 0.08$). NA, not applicable.

HPRT$^-$ sublines exhibited significant morphological differences from the parent line for at least one measure (Fig. 2).

Analysis by single-sample *t*-test to examine the overall effect of HPRT deficiency across all M17 sublines revealed a significant reduction in soma area and a trend toward a reduced soma perimeter (Table 4). Although the number of neurites per cell could not be evaluated by this statistic, neurite length and diameter were not different. Other parameters, such as cell compactness, cell roundness, and neurite branch order were also similar between the M17 parent and the HPRT$^-$ sublines (not shown).

Monoamines

The predominant intracellular monoamine in parent M17 cells was dopamine, with smaller amounts of norepinephrine and serotonin (Table 5). Serotonin and several monoamine metabolites, 3-methoxytyramine (3-MT), homovanillic acid (HVA), and 5-hydroxyindole acetic acid (5-HIAA) were present in conditioned medium.

One-way ANOVA revealed significant differences between the parent and the HPRT$^-$ sublines for each monoamine (Fig. 3). These differences were a combination of increases or decreases in individual HPRT$^-$ sublines. Single-sample *t*-tests indicated that the overall monoaminergic profile of M17 cells was not consistently changed in HPRT deficiency (Table 5).

The expression of several relevant mRNA transcripts including tyrosine hydroxylase, DOPA decarboxylase (DDC), catechol-O-methyltransferase, and vesicular monoamine transporter 2 was determined by quantitative PCR.

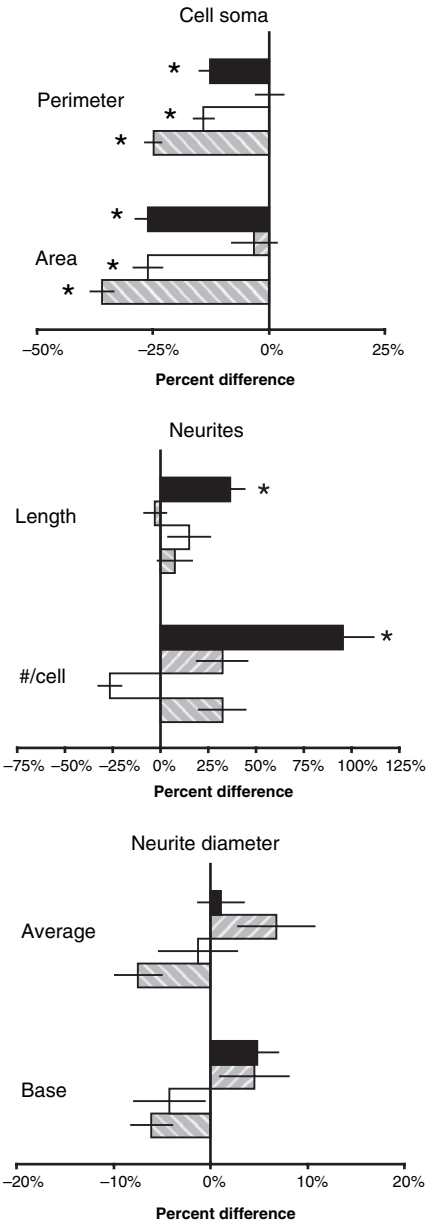

Fig. 2 Quantitative morphological parameters of HPRT$^-$ sublines. Each panel depicts the percent change in the measured parameter for each of the HPRT$^-$ sublines (■, $M17^{TG1}$, ▨, $M17^{TG3}$, □, $M17^{TG6}$, and ▧, $M17^{TG8}$) when compared with the M17 parent line. Significant *post hoc* differences by one-way ANOVA are indicated by *, $p < 0.05$. Summary statistics are provided in Table 4.

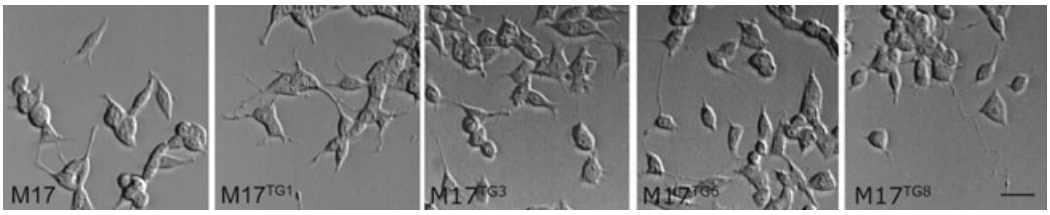

Fig. 1 Phase-contrast micrographs of the parent M17 and HPRT$^-$ sublines; scale bar = 25 μm.

Table 4 Summary statistics for morphological parameters

	Differences among lines (one-way ANOVA)		Differences attributable to HPRT (single-sample *t*-test)		
	F or χ^2	*p*-value	HPRT (+)	HPRT (−)	*p*-value
Soma					
Area (μm^2)	22.3	<0.0001	266.6 ± 9.0	205.9 ± 18.8	0.048
Perimeter (μm)	23.1	<0.0001	67.7 ± 1.4	59.0 ± 3.6	0.095
Neurites					
No. of neurites per cell[a]	46.7	<0.0001	0.7 ± 0.1	0.9 ± 0.2	–
Overall length (μm)	6.5	<0.0001	12.6 ± 1.0	14.0 ± 1.1	0.327
Average diameter (μm)	2.9	0.021	2.0 ± 0.1	2.0 ± 0.1	0.938
Base diameter (μm)	2.5	0.042	2.5 ± 0.1	2.5 ± 0.1	0.955

M17 parent line and HPRT$^-$ sublines (±SEM). Differences among lines were determined by one-way ANOVA. Significant *post hoc t*-test differences between the parent and individual M17 sublines are indicated by * in Fig. 2. Overall differences attributable to HPRT were determined by single-sample *t*-test ($n = 4$).

[a]A non-continuous variable evaluated by Kruskal–Wallis one-way ANOVA, but insufficient *n* for analysis by a non-parametric equivalent of the single-sample *t*-test.

Table 5 Summary statistics for monoamines

	Differences among lines (one-way ANOVA)		Differences attributable to HPRT (single-sample *t*-test)		
	F	*p*-value	HPRT (+)	HPRT (−)	*p*-value
Intracellular					
NE	151.0	<0.0001	2.4 ± 0.1	3.7 ± 1.7	0.487
DA	181.7	<0.0001	19.7 ± 0.6	34.9 ± 8.4	0.167
5-HT	327.5	<0.0001	8.1 ± 0.3	16.2 ± 16.2	0.650
Extracellular					
DOPAC	294.6	<0.0001	ND	26.6 ± 10.0	0.076
3-MT	43.2	<0.0001	1439.1 ± 110.1	1510.0 ± 304.7	0.831
HVA	117.0	<0.0001	453.9 ± 34.4	863.7 ± 235.1	0.180
5-HT	34.0	<0.0001	41.2 ± 2.9	68.7 ± 12.7	0.119
5-HIAA	35.4	<0.0001	164.7 ± 11.7	274.2 ± 58.7	0.159
mRNA					
TH	103.5	<0.0001	1.0 ± 0.0	1.2 ± 0.3	0.650
DDC	13.9	<0.0001	1.0 ± 0.2	0.4 ± 0.1	0.007
VMAT2	135.4	<0.0001	0.8 ± 0.0	0.6 ± 0.2	0.532
COMT	49.1	<0.0001	1.5 ± 0.1	1.5 ± 0.3	0.337

Monoamines (ng/mg cell protein ±SEM) in the M17 parent line and HPRT$^-$ sublines, as well as mRNA expression (relative units normalized to GAPDH SEM). Differences among lines were determined by one-way ANOVA. Significant *post hoc t*-test differences between the parent and individual M17 sublines are indicated by * in Fig. 3. Overall differences attributable to HPRT were determined by single-sample *t*-test ($n = 4$). ND, not detected.

Significant differences existed for individual sublines by one-way ANOVA (Fig. 3). Only DDC expression was consistently decreased in the HPRT$^-$ M17 sublines as determined by single-sample *t*-test (Table 5). Expression levels of several other transcripts, including the dopamine transporter and monoamine oxidase B, were too low to measure.

Purines

Significant media accumulation of hypoxanthine, guanine, and xanthine was observed in all of the HPRT$^-$ sublines (Fig. 4). This difference in extracellular purines was significant by both one-way ANOVA and single-sample *t*-test (Table 6).

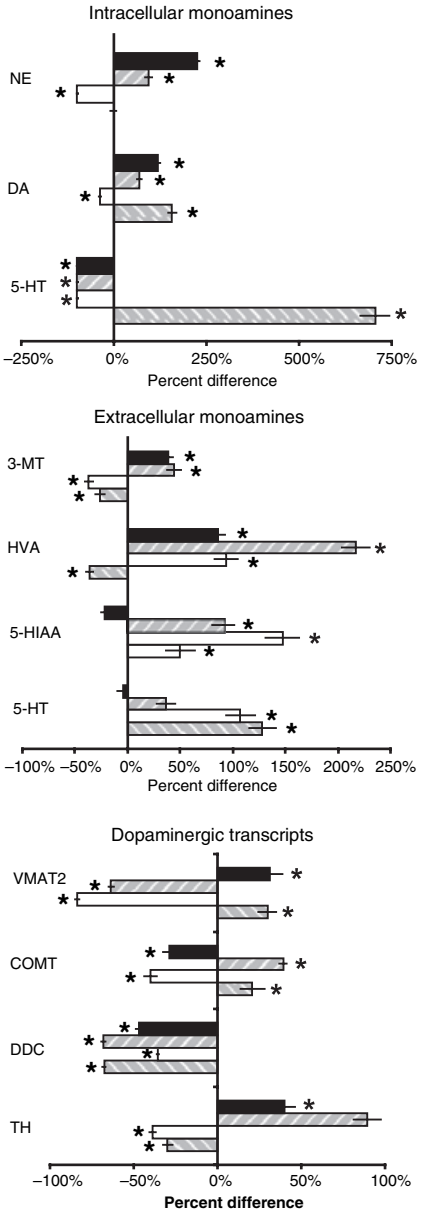

Fig. 3 Monoamines and related mRNA transcripts in HPRT$^-$ M17 sublines. Each panel depicts the percent change in the measured analyte for each of the HPRT$^-$ sublines (■, M17^{TG1}, ▨, M17^{TG3}, □, M17^{TG6}, and ▧, M17^{TG8}) when compared with the M17 parent line. Significant *post hoc* differences by ANOVA are indicated by *, $p < 0.05$. Summary statistics are provided in Table 5. DOPAC was detected in the media from three of the four sublines, but not in the parent.

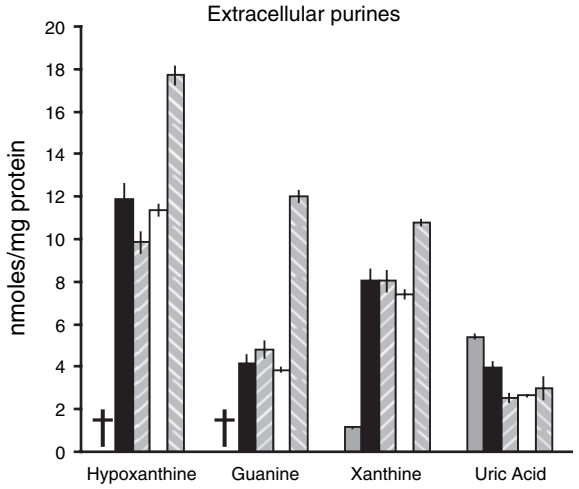

Fig. 4 Extracellular purines in conditioned media of the parent M17 (▩) and each of the HPRT$^-$ M17 sublines (■, M17^{TG1}, ▨, M17^{TG3}, □, M17^{TG6}, and ▧, M17^{TG8}). A significant increase in hypoxanthine, guanine, and xanthine and a significant decrease in uric acid was observed in the media of all four HPRT$^-$ sublines by both ANOVA and single-sample *t*-test. † not detected in the parent line. Summary statistics are provided in Table 6.

Intracellular purines were evaluated in four separate experiments. The magnitude of change for specific nucleotides was often small and did not achieve statistical significance in every experiment, but changes in guanine nucleotides were frequent. To increase the statistical power of the analysis, the data from each of the four separate experiments were combined in a single large analysis. By this approach, significant differences between the parent line and individual HPRT$^-$ cell lines were found by one-way ANOVA (Fig. 5), most notably decreased GTP and increased GDP. These changes were also reflected in the single-sample *t*-test analysis of the overall effect of HPRT deficiency, where trends toward reduced GTP and increased GDP levels were observed (Table 6). Adenine nucleotides were normal.

The physiological relevance of perturbations in purine nucleotide pools may depend on relative changes in nucleotide species. Therefore, several derived variables, including nucleotide ratios and adenylate and guanylate energy charges (AEC and GEC), were also evaluated. AEC and GEC were calculated using the formula ([NTP] + 0.5 × [NDP])/([NTP] + [NDP] + [NMP]) where N = G or A. This generates a parameter that varies between 0 and 1 (Atkinson and Walton 1967; Atkinson 1968; Walton and Gill 1975). The overall effect of HPRT deficiency by single-sample *t*-test revealed a significant reduction in the GTP : GDP ratio that was also manifested in reduced cellular GEC. The ratio of total adenine to guanine nucleotides was also increased, but no differences in adenine nucleotide ratios were found.

Several pyridines (NAD^+, NADH, and $NADP^+$) and pyrimidine nucleotides (UTP and UDP-glucose) were also detected and quantified. Except for an increase in UTP ($p = 0.004$) and $NADP^+$ ($p = 0.01$), there were no other overall differences between the parent and HPRT$^-$ sublines by single-sample *t*-test (not shown).

Table 6 Summary statistics for purines

	Differences among lines (one-way ANOVA)		Differences attributable to HPRT (single-sample *t*-test)		
	F	*p*-value	HPRT (+)	HPRT (–)	*p*-value
Intracellular purines					
Nucleotides					
ATP	1.8	0.136	33.4 ± 1.7	34.0 ± 1.6	0.724
ADP	0.2	0.947	2.2 ± 0.1	2.2 ± 0.1	0.331
AMP	2.6	0.041	0.1 ± 0.0	0.1 ± 0.0	0.496
Σ ANT	1.2	0.309	33.4 ± 1.4	35.5 ± 1.0	0.139
GTP	3.4	0.012	7.0 ± 0.2	6.3 ± 0.2	0.076
GDP	1.2	0.336	0.5 ± 0.0	0.6 ± 0.0	0.076
GMP	3.3	0.015	0.1 ± 0.0	0.1 ± 0.0	0.250
Σ GNT	2.5	0.049	7.5 ± 0.2	7.2 ± 0.2	0.328
Ratios					
ATP : AMP	5.7	0.001	216.9 ± 14.7	261.0 ± 20.4	0.119
ATP : ADP	1.9	0.121	14.9 ± 0.5	15.6 ± 0.6	0.318
AEC	2.7	0.039	0.963 ± 0.0	0.967 ± 0.0	0.354
GTP : GMP	0.7	0.599	96.8 ± 9.6	131.4 ± 17.0	0.136
GTP : GDP	0.3	0.902	14.9 ± 1.0	13.2 ± 0.4	0.025
GEC	2.1	0.093	0.955 ± 0.0	0.943 ± 0.0	0.028
A : G	1.7	0.166	4.5 ± 0.1	4.9 ± 0.1	0.005
Extracellular purines					
Hypoxanthine	207.8	<0.0001	ND	12.7 ± 1.7	0.005
Guanine	282.8	<0.0001	ND	6.2 ± 1.9	0.049
Xanthine	114.0	<0.0001	1.2 ± 0.0	8.6 ± 0.8	0.002
Uric acid	18.9	<0.0001	5.4 ± 0.1	3.0 ± 0.3	0.005

Purines (ng/mg cell protein ± SEM) in the M17 parent line and HPRT$^-$ sublines (combined data from four independent experiments). Differences among lines were determined by one-way ANOVA. Significant *post hoc t*-test differences between the parent and individual M17 sublines are indicated by * in Fig. 5. Extracellular purines (Fig. 4) were significantly different from the parent in each of the M17 sublines. Overall differences attributable to HPRT were determined by single-sample *t*-test ($n = 4$). ND, not detected; Σ ANT, total adenine nucleotides; Σ GNT, total guanine nucleotides; AEC, adenylate energy charge; GEC, guanylate energy charge; A : G, ratio of Σ ANT to Σ GNT.

Discussion

Utilizing a TFO-mediated gene-targeting strategy, we isolated four HPRT$^-$ sublines of the human dopaminergic neuroblastoma, SK-N-BE(2) M17. As predicted, each of these sublines had a small deletion in the HPRT gene encompassing all or part of exon 5. Substantial variation among individual sublines was observed for most biochemical and some morphological features. Despite this variation, these HPRT$^-$ sublines showed several overall significant abnormalities when analyzed as a group. First, HPRT$^-$ sublines universally failed to incorporate hypoxanthine with its subsequent accumulation, along with guanine and xanthine, in the culture media. Second, the GEC and the GTP : GDP ratio in HPRT$^-$ sublines were significantly reduced, but adenine nucleotides were normal. Third, UTP and $NADP^+$ levels were significantly increased. Fourth, DDC mRNA transcript levels were consistently reduced in the HPRT$^-$ sublines, while monoamines were normal. Fifth, HPRT$^-$ cells were significantly smaller in size. These cells provide a valuable new model for the study of LND that is human-derived, neuron-like, and dopaminergic. In addition, these results provide more general insights into differing results obtained in prior culture models of LND.

Tissue culture models have been valuable for studying the effects of lost HPRT activity. Increased *de novo* purine synthesis, accumulation of phosphoribosylpyrophosphate and hypoxanthine, and increased adenine phosphoribosyltransferase activity have frequently been observed in a number of studies of HPRT$^-$ cells (Jinnah and Friedmann 2000). The consistency of such findings increases confidence that they are as a result of HPRT deficiency (Jinnah *et al.* 2000). In contrast, many additional morphological and biochemical changes have been attributed to a loss of HPRT function in one or a few studies (Table 7). The reasons for this lack of consistency are unclear and this has made it difficult to determine which processes might be physiologically relevant in HPRT deficiency. It has been suggested that species differences, particularly between rodents and humans, are responsible for the inconsistency (Pinto *et al.*

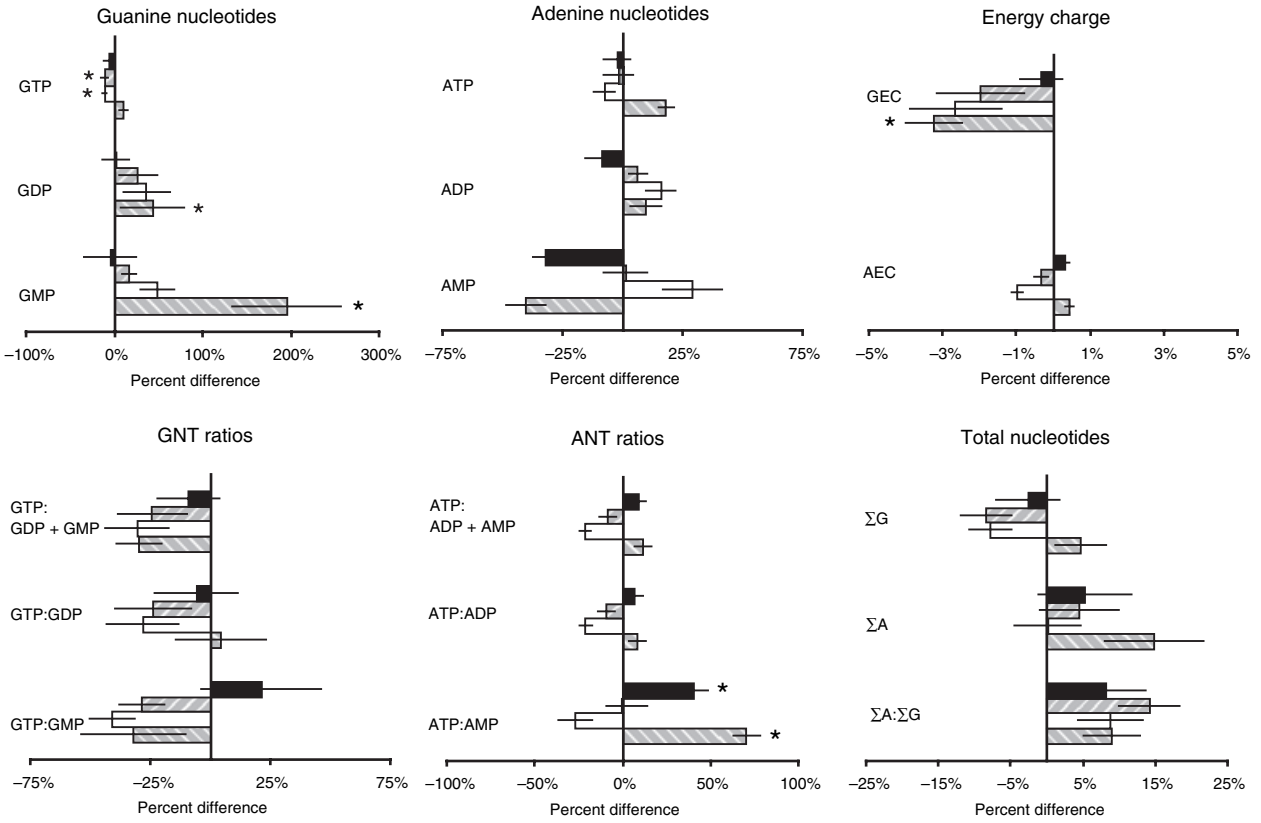

Fig. 5 Purines in HPRT$^-$ sublines. Each panel depicts the percent change in the measured analyte for each of the HPRT$^-$ sublines (■, M17^{TG1}, ▨, M17^{TG3}, □, M17^{TG6}, and ▧, M17^{TG8}) when compared with the M17 parent line. Significant *post hoc* differences by ANOVA indicated by *, $p < 0.05$. Summary statistics are provided in Table 6.

2005). Others have argued that the manifestations of HPRT deficiency vary according to cell type (Pelled *et al*. 1999). Both are probably contributing factors.

Our results highlight another important source of variability. Many of the cell lines used to make HPRT$^-$ models, including the M17 cells used in this study, consist of mixed populations. Individual sublines derived from heterogeneous populations may exhibit idiosyncratic properties that differ from the parent line, yet are independent of HPRT status (Koike and Takashima 1984; Ciccarone *et al*. 1989; Clementi *et al*. 1992). As many prior studies compared only a single HPRT$^-$ subline with a single control, the diverse findings in the literature may reflect idiosyncratic properties of the subline being studied rather than defects attributable to the lack of HPRT. An experimental approach based on a concurrent analysis of multiple cell lines is a safer strategy for diminishing the influence of singular cell properties and identifying those that are consistent.

A potential alternative for addressing the relevance of findings in HPRT deficiency would be to restore enzyme function by transfection or viral vector-mediated methods. Those abnormalities that are rescued could then be more confidently ascribed to the loss of HPRT. Unfortunately, this approach may be unreliable for two reasons. First, it assumes that the abnormality in question is reversible. This assumption may not be valid for changes in developmental fate, which are often irreversible. This issue is particularly relevant for studies of neuroblastoma lines. Second, stably transfected sublines are likely to express the same variability inherent in the original population, necessitating simultaneous evaluation of multiple revertants. The evaluation of multiple revertants for each subline rapidly becomes logistically untenable.

Most investigators believe that the loss of HPRT activity and purine salvage leads to the neurobehavioral syndrome of LND by adversely impacting purine homeostasis. In a review of the literature, we identified 21 unique studies that report on the purine content of HPRT$^-$ cells (Table 7). Seventeen of these studies were performed in cells derived from LND patients such as erythrocytes, platelets, lymphocytes, and fibroblasts. The remaining studies utilized rodent cell lines or primary cultures from rodent brain. There is only limited consensus among these studies as to what changes in purine nucleotide pools can be attributed to loss of purine salvage. In some instances, reported changes are not confirmed by statistical methods or rely on historical controls. Of these

Table 7 Reported purine changes in HPRT$^-$ cells

Species	Cell	#	ATP	ADP	AMP	GTP	GDP	GMP	Other	Reference
Human	RBC	2	↓	↓	↓	U	–	–	–	Lommen *et al.* (1971)
Human	RBC	3	↑	↑	U	–	–	–	↑ATP : AMP, ↑total	Nuki *et al.* (1977b)
Human	RBC	5	U	U	–	↓	U	–	–	Sidi and Mitchell (1985)
Human	RBC	2	U	U	–	↓	↓	–	–	Simmonds *et al.* (1987); Simmonds *et al.* (1988)
Human	RBC	6	↓	–	–	↓	–	–	–	Harkness and McCreanor (1991)
Human	RBC	10	U	–	–	↓	–	–	–	Micheli *et al.* (1999)
Human	Platelets	3	↓	U	–	–	–	–	↓ATP : ADP	Rivard *et al.* (1975)
Human	LB	1	U	U	U	U	U	–	–	Brenton *et al.* (1977)
Human	LB	1–2	U	U	U	U	U	U	–	Nuki *et al.* (1977b)
Human	LB	NS	U	U	U	U	U	U	–	Nuki *et al.* (1977a)
Human	LB	1	↓	–	–	–	–	–	↓ATP : GTP	Willis *et al.* (1984)
Human	LB	11	↓	U	U		U		AEC = U, ↓total A	McCreanor *et al.* (1986)
Human	LB	3	U	–	–	U	–	–	–	Becker *et al.* (1992)
Human	LB	5	↓	–	–	–	–	–	–	McCreanor (1989); McCreanor and Harkness (1995)
Human	FB	4	–	–	–	U	–	–	total = U	Rosenbloom (1968)
Human	FB	1	–	–	–	–	–	–	↑ATP : ADP, total = U	Nuki *et al.* (1977b)
Human	FB	2	U	–	–	U	–	–	–	Becker and Kim (1987); Becker *et al.* (1987)
Human	FB	4	↑	–	–	↑	↑	–	AEC = U	Hussain *et al.* (1999)
Human	FB	8	↓	–	–		–	–	AEC = U	Fairbanks *et al.* (2002)
Mouse	NB	1	–	↑	↑	–	↑	↑	↓AEC	Snyder *et al.* (1978)
Mouse	Glia	NS	↓	↓	–		U	–	–	Pelled *et al.* (1999); Brosh *et al.* (2000); Zoref-Shani *et al.* (2001)
Mouse	Neuron	NS	U	–	–	U	–	–	–	Brosh *et al.* (2000); Zoref-Shani *et al.* (2001)
Rat	Neuroma	1	U	U	–	U	U	–	–	Zoref-Shani *et al.* (1993); Brosh *et al.* (2000); Zoref-Shani *et al.* (2001)

Cell types: RBC, erythrocytes; LB, lymphoblasts; FB, fibroblasts; NB, neuroblastomas; #, the number of patient samples or independent cell lines studied; NS, not specified; U, unchanged.

reports, four reported a decrease in adenine nucleotides, three reported a decrease in guanine nucleotides, and four reported a decrease in both. Nine studies, on the contrary, observed no change in either guanine or adenine nucleotide content. There are three reports of increased nucleotide content in HPRT deficiency, one for adenine nucleotides and two for both adenine and guanine nucleotides. A more consistent pattern is evident among the 14 studies in the literature that report the effects of HPRT deficiency on pyrimidine nucleotide pools, especially increased UTP levels. Similarly, the nine studies that describe pyridine content frequently reported elevated NAD^+ levels (Table 8).

Our results confirm that significant variability may occur in one or more purine nucleotides in HPRT$^-$ cells. Much of this variability appears to be idiosyncratic as it was inconsistent across sublines. This variability suggests that different cells may maintain purine pools at different levels. Despite this variability, aggregate comparisons across sublines showed a significant change only in guanine nucleotides. We found that HPRT$^-$ cells exhibited a significant decrease in GTP : GDP ratio and GEC, a measure of relative energy storage as anhydride-bound phosphate in guanine nucleotides. This was not an effect of reduced nucleotide phosphorylation in HPRT$^-$ lines as adenine nucleotide ratios and AEC were unaffected. Even small changes in guanine nucleotide ratios may impact the multitude of GTP-dependent processes and may be an important regulatory strategy as has been suggested for eIF-2 phosphatase activity (Safer and Jagus 1979). Consistent with this notion, Pinto *et al*. recently reported changes in GTPase function in several HPRT$^-$ cell lines (Pinto *et al*. 2005).

Many studies, including seven of eight studies in Tables 7 and 8, have shown increases in *de novo* synthesis, some with dramatic elevations of 10-fold or more (Zoref *et al*. 1978;

Table 8 Reported pyrimidine and pyridine changes in HPRT$^-$ cells

Species	Cell	#	UTP	UDP	CTP	NAD+	NADH	NADP+	NADPH	Other	Reference
Human	RBC	3	↑	–	–	–	–	–	–	↑UMP, ↑total, ↑UDPG	Nuki *et al.* (1977b)
Human	RBC	5	–	–	–	–	–	–	–	+ZTP	Sidi and Mitchell (1985)
Human	RBC	2	–	–	–	↑	–	–	–	↑UDPG, +ZTP	Simmonds *et al.* (1987); Simmonds *et al.* (1988)
Human	RBC	2	–	–	–	↑	U	U	U		Micheli *et al.* (1993)
Human	RBC	4	–	–	–	↑	–	–	–		Sestini *et al.* (1998)
Human	RBC	10	–	–	–	↑	–	U	–	↑UDP-sugars	Micheli *et al.* (1999)
Human	RBC	16	–	–	–	↑	–	–	–		Bertelli *et al.* (2004)
Human	LB	NS	↑	↑	↑	–	–	–	–		Nuki *et al.* (1977a)
Human	LB	1–2	↑	↑	↑	–	–	–	–	↑UDP-sugars	Nuki *et al.* (1977b)
Human	LB	1	↑	–	↑	–	–	–	–	↑Total U/C	Brenton *et al.* (1977)
Human	LB	5	–	–	–	U	U	U	U		McCreanor and Harkness (1995)
Human	FB	1	–	–	–	–	–	–	–	Total U/C = U	Nuki *et al.* (1977b)
Human	FB	2	U	–	U	–	–	–	–		Becker *et al.* (1987)
Human	FB	8	U	–	U	↓	–	–	–		Fairbanks *et al.* (2002)
Human	FB	4	↑	–	↑	↑	–	–	–		Hussain *et al.* (1999)
Mouse	NB	1	U	–	U	U	–	–	–	↑UDP-sugars	Snyder *et al.* (1978)
Mouse	Neuron	NS	↑	–	↑	–	–	–	–	↑UTP/ATP, ↑UTP/GTP, ↑CTP/ATP	Brosh *et al.* (2000); Zoref-Shani *et al.* (2001)
Mouse	Glia	1	↑	–	U	–	–	–	–	↑UTP:ATP, ↑UTP:GTP	Pelled *et al.* (1999); Brosh *et al.* (2000); Zoref-Shani *et al.* (2001)
Rat	Neuroma	1	↑	–	–	–	–	–	–	No Z nuc	Zoref-Shani *et al.* (1993); Brosh *et al.* (2000); Zoref-Shani *et al.* (2001)

Cell types: RBC, erythrocytes; LB, lymphoblasts; FB, fibroblasts; NB, neuroblastomas; #, the number of patient samples or independent cell lines studied; NS, not specified; U, unchanged; Z nuc, Z-nucleotides.

Zoref-Shani and Sperling 1980). A surprising finding in our study was the normal rate of *de novo* purine synthesis in the HPRT$^-$ cell lines, which ranged from 0.6- to 2-fold that of the parent line. This might be a limitation of the methodology employed. Given increased media levels of guanine, hypoxanthine, and xanthine in HPRT$^-$ lines, rapid degradation, and excretion of newly synthesized purines during the 90-min assay could have led to an underestimation of *de novo* synthesis rate. The lack of consistent change in purine synthesis in our lines could also reflect species differences or culture conditions, as suggested by others (Southgate *et al.* 2000). Another possibility is that neuron-like cells do not exhibit this aspect of HPRT deficiency.

Another surprising finding was the lack of change in dopamine and its metabolites in HPRT$^-$ M17 neuroblastomas. Humans with LND have nearly a 75% reduction in striatal dopamine and a 50% reduction in striatal dopamine is reported for HPRT$^-$ mice (Lloyd *et al.* 1981; Finger *et al.* 1988; Dunnett *et al.* 1989; Jinnah *et al.* 1994; Jinnah *et al.* 1999; Saito *et al.* 1999). Similarly, decreased cellular dopamine is found in the two published tissue culture models where dopamine has been measured, primary cultures from HPRT$^-$ mice (Boer *et al.* 2001; Smith and Friedmann 2004) and 6TG-resistant PC12 cells (Bitler and Howard 1986). Several studies have reported reductions in monoamine oxidase activity (Breakefield *et al.* 1976; Skaper and Seegmiller 1976). Although it was expected that dopamine loss would also be recapitulated in dopaminergic M17 neuroblastomas, intracellular dopamine was not consistently altered in the HPRT$^-$ sublines.

One possible explanation is the source of M17 neuroblastomas. One of the hallmarks of LND and HPRT$^-$ mice is the specificity of dopamine deficit and its restriction to nigrostriatal neurons (Lloyd *et al.* 1981; Jinnah *et al.* 1994). Other dopaminergic neurons, such as olfactory interneurons, and other neurotransmitter systems are spared. As a neural crest derivative, M17 cells may not exhibit the same loss of dopamine as nigrostriatal neurons. A second possibility is that the down-regulation of DDC expression is common to both M17 cells and nigrostriatal neurons and directly attributable to defects in HPRT, but only manifest as dopamine loss *in vivo* because of environmental or regulatory factors.

In addition to biochemical abnormalities, impaired function of dopaminergic neurons as a result of anatomical aberrations is a potential consequence of HPRT deficiency in LND (Jinnah *et al.* 2006). A limited number of reports directly address morphological parameters of HPRT$^-$ cell

lines, but with few consistent findings (Connolly 2001b; Connolly *et al*. 2001). Several studies describe a lack of overt morphological abnormalities; often without quantitative assessment (Bitler and Howard 1986; Porter and Fournier 1996; Smith and Friedmann 2004).

There are two reports of dopamine neurons in primary cultures from HPRT$^-$ mice. In one, HPRT$^-$ dopamine neurons exhibited reduced dendritic length, compared with HPRT-competent neurons (Boer *et al*. 2001). In contrast, a second study found no morphological differences (Smith and Friedmann 2004). The reason for this discrepancy remains unclear. In each of the single HPRT$^-$ sublines of the rodent neuroblastomas N2a and B103, neurite outgrowth was reported to be enhanced (Connolly 2001a; Connolly *et al*. 2001), as measured by increased neurite number or neurite length. This was accompanied by larger cell soma and decreased proliferation rates. HPRT$^-$ PC12 cells, on the contrary, lacked overt morphological abnormalities in one study (Bitler and Howard 1986), although a quantitative morphological assessment was not performed. In a second study, HPRT$^-$ PC12 cells lacked neurites, but retained short processes (Connolly 2001b). Impaired neurite extension in response to nerve growth factor differentiation has also been reported in HPRT$^-$ PC12 cells (Yeh *et al*. 1998; Connolly 2001b), although this was limited to two of four sublines (Yeh *et al*. 1998).

We also found morphological changes in HPRT$^-$ M17 cells, most consistently a reduction in cell size. Morphological abnormalities could be a consequence of the alteration in GTP : GDP ratio. Rho family GTPases, whose activity is GTP/GDP-dependent, are essential modulators of neurite initiation, extension, branching, and spine formation in neurons (Govek *et al*. 2005; Negishi and Katoh 2005). Other small GTPases regulate the cell cycle and cell division (Welsh 2004). An abnormality affecting the synchronization between cell growth and cell division could result in abnormally large or small cells. Abnormal GTPase function in affected patients could therefore cause neurobehavioral abnormalities via disturbed neuronal development.

The SK-N-BE(2) M17 neuroblastoma studies presented here describe a new human, tissue culture model for LND. The importance of these observations lies in the use of a human, neuron-like cell and the analysis of multiple, independent HPRT$^-$ sublines. Reliance on any single HPRT$^-$ subline would have provided a number of significant morphological or biochemical changes with respect to the parent line, but our findings that were consistent across all sublines are most likely to have relevance for the pathophysiology of LND. This cellular model demonstrates that HPRT-mediated purine recycling has a significant influence on the maintenance of guanine nucleotide ratios without a similar impact on adenine nucleotide pools or total guanine nucleotide content. These HPRT$^-$ cells exhibit changes in cell soma size in the absence of consistent changes in monoamine content or indicators of impaired viability. These results provide additional evidence that impaired guanine recycling may be the relevant biochemical mechanism underlying the neurobehavioral manifestations of LND, perhaps through dysregulation of small GTPases.

Acknowledgements

This research was supported by an NIH grant (HD39795) and F32 fellowship (NS052040), the Lesch-Nyhan Syndrome Children's Research Foundation, the Association Lesch-Nyhan Action, and the Fondation Jérôme Lejeune.

References

Atkinson D. E. (1968) The energy charge of the adenylate pool as a regulatory parameter. Interaction with feedback modifiers. *Biochemistry* **7**, 4030–4034.

Atkinson D. E. and Walton G. M. (1967) Adenosine triphosphate conservation in metabolic regulation. Rat liver citrate cleavage enzyme. *J. Biol. Chem.* **242**, 3239–3241.

Baptista M. J., O'Farrell C., Daya S., Ahmad R., Miller D. W., Hardy J., Farrer M. J. and Cookson M. R. (2003) Co-ordinate transcriptional regulation of dopamine synthesis genes by alpha-synuclein in human neuroblastoma cell lines. *J. Neurochem.* **85**, 957–968.

Becker M. A. and Kim M. (1987) Regulation of purine synthesis de novo in human fibroblasts by purine nucleotides and phosphoribosylpyrophosphate. *J. Biol. Chem.* **262**, 14 531–14 537.

Becker M. A., Losman M. J. and Kim M. (1987) Mechanisms of accelerated purine nucleotide synthesis in human fibroblasts with superactive phosphoribosylpyrophosphate synthetases. *J. Biol. Chem.* **262**, 5596–5602.

Becker M. A., Kim M., Husain K. and Kang T. (1992) Regulation of purine nucleotide synthesis in human B lymphoblasts with both hypoxanthine–guanine phosphoribosyltransferase deficiency and phosphoribosylpyrophosphate synthetase superactivity. *J. Biol. Chem.* **267**, 4317–4321.

Bertelli M., Randi D., Micheli V., Gallo S., Andrighetto G., Parmigiani P., Jacomelli G., Carella M., Lievore C. and Pandolfo M. (2004) Molecular basis of hypoxanthine–guanine phosphoribosyltransferase deficiency in Italian Lesch-Nyhan patients: identification of nine novel mutations. *J. Inherit. Metab. Dis.* **27**, 767–773.

Biedler J. L. and Spengler B. A. (1976) A novel chromosome abnormality in human neuroblastoma and antifolate-resistant Chinese hamster cell lives in culture. *J. Natl Cancer Inst.* **57**, 683–695.

Bitler C. M. and Howard B. D. (1986) Dopamine metabolism in hypoxanthine–guanine phosphoribosyltransferase-deficient variants of PC12 cells. *J. Neurochem.* **47**, 107–112.

Boer P., Brosh S., Wasserman L., Hammel I., Zoref-Shani E. and Sperling O. (2001) Decelerated rate of dendrite outgrowth from dopaminergic neurons in primary cultures from brains of hypoxanthine phosphoribosyltransferase-deficient knockout mice. *Neurosci. Lett.* **303**, 45–48.

Breakefield X. O., Castiglione C. M. and Edelstein S. B. (1976) Monoamine oxidase activity decreased in cells lacking hypoxanthine phosphoribosyltransferase activity. *Science* **192**, 1018–1020.

Brenton D. P., Astrin K. H., Cruikshank M. K. and Seegmiller J. E. (1977) Measurement of free nucleotides in cultured human lymphoid cells using high pressure liquid chromatography. *Biochem. Med.* **17**, 231–247.

Brosh S., Boer P., Sperling O. and Zoref-Shani E. (2000) Elevated UTP and CTP content in cultured neurons from HPRT-deficient transgenic mice. *J. Mol. Neurosci.* **14**, 87–91.

Ciccarone V., Spengler B. A., Meyers M. B., Biedler J. L. and Ross R. A. (1989) Phenotypic diversification in human neuroblastoma cells: expression of distinct neural crest lineages. *Cancer Res.* **49**, 219–225.

Clementi E., Racchetti G., Zacchetti D., Panzeri M. C. and Meldolesi J. (1992) Differential expression of markers and activities in a group of PC12 nerve cell clones. *Eur. J. Neurosci.* **4**, 944–953.

Connolly G. P. (2001a) Hypoxanthine–guanine phosphoribosyltransferase-deficiency produces aberrant neurite outgrowth of rodent neuroblastoma used to model the neurological disorder Lesch Nyhan syndrome. *Neurosci. Lett.* **314**, 61–64.

Connolly G. P. (2001b) Cell imaging and morphology: application to studies of inherited purine metabolic disorders. *Pharmacol. Ther.* **90**, 267–281.

Connolly G. P., Duley J. A. and Stacey N. C. (2001) Abnormal development of hypoxanthine–guanine phosphoribosyltransferase-deficient CNS neuroblastoma. *Brain Res.* **918**, 20–27.

Dunnett S. B., Sirinathsinghji D. J., Heavens R., Rogers D. C. and Kuehn M. R. (1989) Monoamine deficiency in a transgenic (Hprt-) mouse model of Lesch-Nyhan syndrome. *Brain Res.* **501**, 401–406.

Fairbanks L. D., Jacomelli G., Micheli V., Slade T. and Simmonds H. A. (2002) Severe pyridine nucleotide depletion in fibroblasts from Lesch-Nyhan patients. *Biochem. J.* **366**, 265–272.

Finger S., Heavens R. P., Sirinathsinghji D. J., Kuehn M. R. and Dunnett S. B. (1988) Behavioral and neurochemical evaluation of a transgenic mouse model of Lesch-Nyhan syndrome. *J. Neurol. Sci.* **86**, 203–213.

Freshney R. (2000) *Culture of Animal Cells; A Manual of Basic Technique*, 4th Edn, p. 577. A John Wiley & Sons, Inc., Publication, New York.

Furth E. E., Thilly W. G., Penman B. W., Liber H. L. and Rand W. M. (1981) Quantitative assay for mutation in diploid human lymphoblasts using microtiter plates. *Anal. Biochem.* **110**, 1–8.

Govek E. E., Newey S. E. and Van Aelst L. (2005) The role of the Rho GTPases in neuronal development. *Genes Dev.* **19**, 1–49.

Harkness R. A. and McCreanor G. M. (1991) Erythrocyte nucleotide variations in hypoxanthine phosphoribosyltransferase deficiency. *J. Inherit. Metab. Dis.* **14**, 848–849.

Hussain S. P., Duley J. A. and Connolly G. P. (1999) Purine and pyrimidine levels in cultured skin fibroblasts from control and Lesch-Nyhan patients. *Cell. Mol. Biol. Lett.* **4**, 377–378.

Jinnah H. and Friedmann T. (2000) Lesch-Nyhan disease and its variants, in *The Metabolic and Molecular Basis of Inherited Disease* (Scriver C., Beaudet A., Sly W. and Valle D., eds.), pp. 2537–2570. McGraw-Hill, New York.

Jinnah H. A., Wojcik B. E., Hunt M., Narang N., Lee K. Y., Goldstein M., Wamsley J. K., Langlais P. J. and Friedmann T. (1994) Dopamine deficiency in a genetic mouse model of Lesch-Nyhan disease. *J. Neurosci.* **14**, 1164–1175.

Jinnah H. A., Jones M. D., Wojcik B. E., Rothstein J. D., Hess E. J., Friedmann T. and Breese G. R. (1999) Influence of age and strain on striatal dopamine loss in a genetic mouse model of Lesch-Nyhan disease. *J. Neurochem.* **72**, 225–229.

Jinnah H. A., De Gregorio L., Harris J. C., Nyhan W. L. and O'Neill J. P. (2000) The spectrum of inherited mutations causing HPRT deficiency: 75 new cases and a review of 196 previously reported cases. *Mutat. Res.* **463**, 309–326.

Jinnah H. A., Visser J. E., Harris J. C., *et al.* (2006) Delineation of the motor disorder of Lesch-Nyhan disease. *Brain* **129**, 1201–1217.

Koike T. and Takashima A. (1984) Clonal variability of PC12 pheochromocytoma cells with respect to catecholamine biosynthesis. *J. Neurochem.* **42**, 1472–1475.

Lloyd K. G., Hornykiewicz O., Davidson L., Shannak K., Farley I., Goldstein M., Shibuya M., Kelley W. N. and Fox I. H. (1981) Biochemical evidence of dysfunction of brain neurotransmitters in the Lesch-Nyhan syndrome. *N. Engl. J. Med.* **305**, 1106–1111.

Lommen E. J., Vogels G. D., van der Zee S. P., Trijbels J. M. and Schretlen E. D. (1971) Concentration of purine nucleotides in erythrocytes of patients with the Lesch-Nyhan syndrome before and during oral administration of adenine. *Acta Paediatr. Scand.* **60**, 642–646.

McCreanor G. M. (1989) Reduced purine nucleotide content and poly(ADP-ribose) synthetase activity in HPRT-deficient human lymphoblasts. *Adv. Exp. Med. Biol.* **253B**, 243–249.

McCreanor G. M. and Harkness R. A. (1995) Lesch-Nyhan syndrome and its pathogenesis: normal nicotinamide-adenine dinucleotide but reduced ATP concentrations that correlate with reduced poly(ADP-ribose) synthetase activity in HPRT-deficient lymphoblasts. *J. Inherit. Metab. Dis.* **18**, 737–747.

McCreanor G. M., Harkness R. A. and Watts R. W. E. (1986) Reduced concentrations of purine nucleotides in hypoxanthine phosphoribosyltransferase-deficient human lymphoblasts, in *Meeting Biochemical Society*, pp. 555–556. London, England.

Micheli V., Simmonds H. A., Bari M. and Pompucci G. (1993) HPLC determination of oxidized and reduced pyridine coenzymes in human erythrocytes. *Clin. Chim. Acta* **220**, 1–17.

Micheli V., Sestini S., Rocchigiani M., Jacomelli G., Manzoni F., Peruzzi L., Gathof B. S., Zammarchi E. and Pompucci G. (1999) Hypoxanthine–guanine phosphoribosyltransferase deficiency and erythrocyte synthesis of pyridine coenzymes. *Life Sci.* **64**, 2479–2487.

Negishi M. and Katoh H. (2005) Rho family GTPases and dendrite plasticity. *Neuroscientist* **11**, 187–191.

Nuki G., Astrin K., Brenton D., Cruikshank M., Lever J. and Seegmiller J. E. (1977a) Purine and pyrimidine nucleotides in some mutant human lymphoblasts. *Ciba Found. Symp.* **48**, 127–143.

Nuki G., Astrin K., Brenton D., Cruikshank M., Lever J. and Seegmiller J. E. (1977b) Purine and pyrimidine nucleotide concentrations in cells with decreased hypoxanthine–guanine–phosphoribosyltransferase (HGPRT) activity. *Adv. Exp. Med. Biol.* **76A**, 326–340.

Pelled D., Sperling O. and Zoref-Shani E. (1999) Abnormal purine and pyrimidine nucleotide content in primary astroglia cultures from hypoxanthine–guanine phosphoribosyltransferase-deficient transgenic mice. *J. Neurochem.* **72**, 1139–1145.

Pinto C. S., Jinnah H. A., Shirley T. L., Nyhan W. L. and Seifert R. (2005) Altered membrane NTPase activity in Lesch-Nyhan disease fibroblasts: comparison with HPRT knockout mice and HPRT-deficient cell lines. *J. Neurochem.* **93**, 1579–1586.

Porter M. B. and Fournier R. E. (1996) Isolation and characterization of HPRT-deficient human hepatoma cells. *Somat. Cell Mol. Genet.* **22**, 341–348.

Puri N., Majumdar A., Cuenoud B., Natt F., Martin P., Boyd A., Miller P. S. and Seidman M. M. (2002) Minimum number of 2′-O-(2-aminoethyl) residues required for gene knockout activity by triple helix forming oligonucleotides. *Biochemistry* **41**, 7716–7724.

Richards S., Liu S. T., Majumdar A., Liu J. L., Nairn R. S., Bernier M., Maher V. and Seidman M. M. (2005) Triplex targeted genomic crosslinks enter separable deletion and base substitution pathways. *Nucleic Acids Res.* **33**, 5382–5393.

Rivard G. E., Izadi P., Lazerson J., McLaren J. D., Parker C. and Fish C. H. (1975) Functional and metabolic studies of platelets from patients with Lesch-Nyhan syndrome. *Br. J. Haematol.* **31**, 245–253.

Rosenbloom F. M. (1968) Possible mechanism for increased purine biosynthesis de novo in Lesch-Nyhan syndrome. *Fed. Proc.* **27**, 1063–1066.

Safer B. and Jagus R. (1979) Control of eIF-2 phosphatase activity in rabbit reticulocyte lysate. *Proc. Natl Acad. Sci. USA.* **76**, 1094–1098.

Saito Y., Ito M., Hanaoka S., Ohama E., Akaboshi S. and Takashima S. (1999) Dopamine receptor upregulation in Lesch-Nyhan syndrome: a postmortem study. *Neuropediatrics* **30**, 66–71.

Schretlen D. J., Harris J. C., Park K. S., Jinnah H. A. and del Pozo N. O. (2001) Neurocognitive functioning in Lesch-Nyhan disease and partial hypoxanthine–guanine phosphoribosyltransferase deficiency. *J. Int. Neuropsychol. Soc.* **7**, 805–812.

Schretlen D. J., Ward J., Meyer S. M., Yun J., Puig J. G., Nyhan W. L., Jinnah H. A. and Harris J. C. (2005) Behavioral aspects of Lesch-Nyhan disease and its variants. *Dev. Med. Child Neurol.* **47**, 673–677.

Sestini S., Micheli V., Rocchigiani M., Jacomelli G., Manzoni F., Gathof B., Hayek G., Cardona F., Zammarchi E. and Pompucci G. (1998) Enzyme activities leading to NAD synthesis in the erythrocytes of HPRT deficient subjects. *Adv. Exp. Med. Biol.* **431**, 181–184.

Sidi Y. and Mitchell B. S. (1985) Z-nucleotide accumulation in erythrocytes from Lesch-Nyhan patients. *J. Clin. Invest.* **76**, 2416–2419.

Simmonds H. A., Fairbanks L. D., Morris G. S., Morgan G., Watson A. R., Timms P. and Singh B. (1987) Central nervous system dysfunction and erythrocyte guanosine triphosphate depletion in purine nucleoside phosphorylase deficiency. *Arch. Dis. Child.* **62**, 385–391.

Simmonds H. A., Fairbanks L. D., Morris G. S., Webster D. R. and Harley E. H. (1988) Altered erythrocyte nucleotide patterns are characteristic of inherited disorders of purine or pyrimidine metabolism. *Clin. Chim. Acta* **171**, 197–210.

Skaper S. D. and Seegmiller J. E. (1976) Hypoxanthine–guanine phosphoribosyltransferase mutant glioma cells: diminished monamine oxidase activity. *Science* **194**, 1171–1173.

Smith D. W. and Friedmann T. (2004) Discrepant effects of culture conditions on survival and function of dopaminergic neurons. *Neuroreport* **15**, 1025–1028.

Snyder F. F., Cruikshank M. K. and Seegmiller J. E. (1978) A comparison of purine metabolism and nucleotide pools in normal and hypoxanthine–guanine phosphoribosyltransferase-deficient neuroblastoma cells. *Biochim. Biophys. Acta* **543**, 556–569.

Southgate T., Bain D., Fairbanks L. D., Morelli A., Larregina A., Simmonds H. A., Castro M. and Lowenstein P. (2000) Adenoviruses encoding HPRT correct the biochemical abnormalities fully only in HPRT-deficient human cell lines: importance of species differences. *Adv. Exp. Med. Biol.* **486**, 35–40.

Visser J. E., Bar P. R. and Jinnah H. A. (2000) Lesch-Nyhan disease and the basal ganglia. *Brain Res. Brain Res. Rev.* **32**, 449–475.

Walton G. M. and Gill G. N. (1975) Nucleotide regulation of a eukaryotic protein synthesis initiation complex. *Biochim. Biophys. Acta* **390**, 231–245.

Welsh C. F. (2004) Rho GTPases as key transducers of proliferative signals in g1 cell cycle regulation. *Breast Cancer Res. Treat.* **84**, 33–42.

Willis R. C., Jolly D. J., Miller A. D., Plent M. M., Esty A. C., Anderson P. J., Chang H. C., Jones O. W., Seegmiller J. E. and Friedmann T. (1984) Partial phenotypic correction of human Lesch-Nyhan (hypoxanthine–guanine phosphoribosyltransferase-deficient) lymphoblasts with a transmissible retroviral vector. *J. Biol. Chem.* **259**, 7842–7849.

Wood A. W., Becker M. A., Minna J. D. and Seegmiller J. E. (1973) Purine metabolism in normal and thioguanine-resistant neuroblastoma. *Proc. Natl Acad. Sci. USA.* **70**, 3880–3883.

Yeh J., Zheng S. and Howard B. D. (1998) Impaired differentiation of HPRT-deficient dopaminergic neurons: a possible mechanism underlying neuronal dysfunction in Lesch-Nyhan syndrome. *J. Neurosci. Res.* **53**, 78–85.

Zoref E., de Vries A. and Sperling O. (1978) Kinetic aspects of purine metabolism in cultured fibroblasts. A comparative study of cells from patients overproducing purines due to HGPRT deficiency and PRPP synthetase superactivity. *Monogr. Hum. Genet.* **10**, 96–99.

Zoref-Shani E. and Sperling O. (1980) Characterization of purine nucleotide metabolism in cultured fibroblasts with deficiency of hypoxanthine–guanine phosphoribosyltransferase and with superactivity of phosphoribosylpyrophosphate synthetase. *Enzyme* **25**, 413–418.

Zoref-Shani E., Bromberg Y., Brosh S., Sidi Y. and Sperling O. (1993) Characterization of the alterations in purine nucleotide metabolism in hypoxanthine–guanine phosphoribosyltransferase-deficient rat neuroma cell line. *J. Neurochem.* **61**, 457–463.

Zoref-Shani E., Boer P., Brosh S., Pelled D., Bromberg Y. and Sperling O. (2001) Purine nucleotide metabolism in cultured neurons and astroglia from HPRT-deficient knockout mice. *Ital. J. Biochem.* **50**, 9–13.

